Aerosol and Air Quality Research

ORIGINAL RESEARCH
https://doi.org/10.4209/aaqr.200637

Study on the Formation of Secondary Organic Aerosol by Ozonolysis of Citral in the Atmosphere

Chenxi Zhang[1,2*], Xuesong Cao[2], Xiaomin Sun[2], Hengjun Peng[3*]

[1] College of Biological and Environmental Engineering, Binzhou University, Binzhou 256600, China
[2] Environment Research Institute, Shandong University, Qingdao 266200, China
[3] Logistics support department, Shandong University, Jinan 250100, China

ABSTRACT

A major research area in atmospheric chemistry focuses on the formation of secondary organic aerosol (SOA), which contains a large variety of low-volatility organic compounds when generated by the ozonolysis of monoterpenes. Thus, we apply quantum chemistry and kinetic calculations to investigate the ozonolysis of citral, which begins with the formation of primary ozonides (POZs) that decompose into Criegee intermediates (CIs). Although CIs have been previously implicated in tropospheric oxidation, the majority are simple compounds for their class, such as $CH_2OO\cdot$ or $CH_3CHOO\cdot$. This study, however, reports on the generation and reaction kinetics of larger CIs, which have been shown to oxidize NO and SO_2 into NO_2 and SO_3, respectively, leading to the production of nitric acid and sulfuric acid. Furthermore, the reactions between these CIs, and H_2O and SO_2 may serve as the dominant mechanism for removing the former from the troposphere, thereby determining the atmospheric CI concentrations. The low-volatility organic compounds potentially arising from the ozonolysis of citral, including aldehydes (–C(=O)H), ketones (–C(=O)–), alcohols (–OH), and hydroperoxides (–OOH), can form SOA through the nucleation, condensation, and/or partitioning of the condensed and gaseous phases.

Keywords: Secondary organic aerosol, Citral, Ozonolysis, Criegee intermediates

Received: November 19, 2020
Revised: February 18, 2021
Accepted: March 2, 2021

* **Corresponding Authors:**
Chenxi Zhang
sdzhangcx@163.com
Hengjun Peng
phj@sdu.edu.cn

Publisher:
Taiwan Association for Aerosol Research
ISSN: 1680-8584 print
ISSN: 2071-1409 online

1 INTRODUCTION

Atmospheric aerosols significantly affect the earth's radiation balance by absorbing and scattering solar radiation, leading to a decrease in atmospheric visibility and contributing to climate change. Moreover, due to the small particle size and large surface area of atmospheric aerosols, they provide a reaction bed for various atmospheric chemical processes and have a direct effect on human health (Oberdorster *et al.*, 2005; Pope and Dockery, 2006). Atmospheric aerosols are mainly classified as either primary aerosols which are directly discharged into the atmosphere by an exhaust source, or secondary aerosols formed in the atmosphere from chemical reaction with gaseous components (Atkinson and Arey, 2003; Hallquist *et al.*, 2009). Secondary organic aerosols (SOAs) are mainly formed from the oxidation processes of volatile organic compounds (VOCs) and account for a significant fraction of ambient tropospheric aerosols (Jimenez *et al.*, 2009).

About 90% of the total global VOCs emissions that lead to SOAs formation come from biological sources, which including isoprene (C_5H_8), monoterpenes ($C_{10}H_{16}$), and sesquiterpenes ($C_{15}H_{24}$) (Guenther *et al.*, 1995; Goldstein and Galbally, 2007; Friedman and Farmer, 2018; Stangl *et al.*, 2019). Monoterpenes have been found to be the largest contributors to organic aerosol during the summer in the southeastern United States, with mean global emissions estimated to be approximately 107.5 TgC per year (Messina *et al.*, 2016; Zhang *et al.*, 2018; Nagori *et al.*, 2019). As monoterpenes are unsaturated, they rapidly react with O_3, OH and NO_3 radicals, with estimated reaction rates for OH and NO_3 radicals with most monoterpenes being larger than 10^{-11} cm^3 $molecules^{-1}$ s^{-1} and in the range of 10^{-19}–10^{-14} cm^3 $molecules^{-1}$ s^{-1} for O_3 with monoterpenes

(Atkinson, 1997; Calogirou *et al.*, 1999; Martínez *et al.*, 1999; Orlando *et al.*, 2000; Oliveira and Bauerfeldt, 2012). Using the 12-h daytime average OH radical concentration of 2×10^6 molecules cm^{-3}, 12-h nighttime average NO_3 radical concentration of 2.5×10^8 molecules cm^{-3} and 24-h average O_3 concentration of 7×10^{11} molecules cm^{-3}, the fast monoterpene ozonolysis reaction can compete with the OH reaction during the day and the NO_3 reaction at night. Therefore, ozonolysis serves as an important monoterpene loss pathway (Orlando *et al.*, 2000; Atkinson and Arey, 2003; Qin *et al.*, 2018). In addition, a large variety of low-volatility organic compounds, including carbonyl compounds (aldehydes and ketones), hydroxyl compounds and organic acids, have been identified in SOAs generated from the ozonolysis of monoterpenes, such as α-pinene, β-pinene, α-phellandrene, limonene, and sabinene (Jacksonet *et al.*, 2016; Sato *et al.*, 2016; Scorch *et al.*, 2017). Therefore, SOAs formation by the oxidation of monoterpenes is mainly dominated by the ozonolysis reaction.

Monoterpenes generally contain 1–3 unsaturated >C=C< double bonds and are highly reactive. The proposed reaction mechanism for monoterpene ozonolysis starts with O_3 addition to C=C double bonds, which lead to the formation of primary ozonide (POZ). The formed POZ will then rapidly decompose to form Criegee intermediates (CIs). Chemically activated CIs may undergo unimolecular decomposition or isomerization, or bimolecular reactions with H_2O, NO and SO_2 (Kleindienst *et al.*, 2006; Jaoui *et al.*, 2008; Lin *et al.*, 2014; Jackson *et al.*, 2017; Almatarneh *et al.*, 2019), with many previous studies reporting the importance of bimolecular reactions for SOA formation.

Neeb *et al.* (1997) found that hydroxymethyl hydroperoxide (HMHP) was the sole product of the reaction between CH_2OO and water H_2O. HMHP can then be rapidly decomposed into low-volatility organic compounds such as methacrolein and methyl vinyl ketone (Sauer *et al.*, 1999). Presto *et al.* (2005) reported SOA yields from the ozonolysis of α-pinene in the presence of NO_x, suggesting that CIs can react with NO, typically resulting in carbonyl and organic nitrate functionality. Mauldin *et al.* (2012) found that the oxidation of SO_2 to H_2SO_4 by CIs leads to an increase in the production of sulfate aerosols in boreal forests. Sipilä *et al.* (2014) also reported that the reaction between SO_2 and CIs formed from monoterpene ozonolysis is an important source of atmospheric sulfate and SOAs. In addition, Ye *et al.* (2018) studied α-pinene and limonene ozonolysis in the presence of SO_2, finding that the reaction of SO_2 with CIs was responsible for altering SOAs yields. Although these experimental studies indicated that bimolecular CIs reactions were related to SOAs formation, the chemical processes behind these interactions are not yet fully understood. Moreover, most theoretical studies have focused on small CIs, especially the simple carbonyl oxide CH_2OO (Aplincourt and Ruiz-López, 2000; Vereecken *et al.*, 2012; Nguyen *et al.*, 2016). Therefore, it is necessary to study the specific mechanism of SOAs formation from large CIs formed from monoterpene ozonolysis.

As a natural acyclic monoterpene, citral is found in a wide variety of plants, such as Indian lemon grass species and *Litsea cubeba*, and can be used as a key ingredient for various chemical products (Rauber *et al.*, 2005; Gil *et al.*, 2007; Saddiq and Khayyat, 2010). Citral (3,7-dimethyl-2,6-octadienal) is a mixture of two isomeric acyclic monoterpene aldehydes, neral and geranial (Fig. 1), caused by *cis-trans* isomerism at the C=C bond near the aldehyde group. In this article, neral was used to theoretically explore the gas-phase ozonolysis of citral in the presence of H_2O, NO and SO_2, providing novel insights on the formation mechanisms of SOAs during monoterpenes ozonolysis and further deepening our understanding of the atmospheric SOAs.

2 COMPUTATIONAL METHODS

All geometric optimizations were performed using the Gaussian 09 program (Frisch *et al.*, 2009). And in each elementary reaction, the geometric parameters of reactants, pre-reactive complex (PRC), intermediates (IMs), transition states (TSs) and products, were optimized using the M06-2X functional with the 6-31+G(d,p) basis set. Zheng *et al.* (2009) calculated the barrier heights of DBH24/08 database using 348 model chemistries, including heavy-atom transfer (HATBH6), nucleophilic substitution (NSBH6), unimolecular and association (UABH6), and hydrogen-transfer (HTBH6) reactions. The selected functional M06-2X/6-31+G(d,p) was proven to be reliable and appropriate for the configuration optimization and thermodynamic calculation of ozonolysis

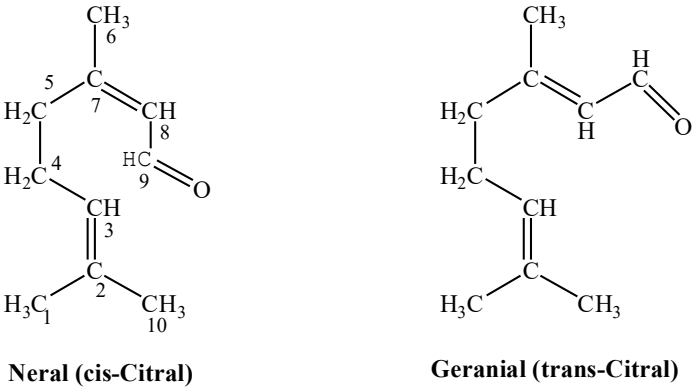

Fig. 1. The structure of neral and geranial.

(Sun *et al.*, 2018; Wang *et al.*, 2019). At the same level of theory, frequency calculations were performed to obtain zero-point energy corrections. The transition states were identified by only one imaginary frequency. More accurate single energies could be obtained using a larger basis set of 6-311++G(3df,3pd).

Using the KiSThelP program (Truhlar *et al.*, 1996; Canneaux *et al.*, 2014), rate constants were calculated using transition-state theory (TST) with Wigner tunneling correction at a pressure of 1.0 bar and 298 K. A scaling factor of 0.967 was applied to the frequency calculated at the M06-2X/6-31+G(d,p) level (Alecu *et al.*, 2010).

When the reaction involved pre-reactive complexes, the reaction rate constants were calculated using the formula described in Eq. (1) (Shiroudi and Deleuze, 2014), as follows:

$$R_1 + R_2 \xleftrightarrow{K_{eq}} R_1 \cdots R_2 \xrightarrow{k_1} IM \tag{1}$$

where K_{eq} represents the equilibrium constant for the first reaction step, R1…R2 means the pre-reactive complexes. The thermodynamic expression of the equilibrium constant for gas-phase reactions is employed in KiSThelP, as described in Eq. (2) as follows:

$$K_{eq} = e^{-\frac{\Delta G^0(T)}{RT}} \tag{2}$$

where $\Delta G^0(T)$ is the associated standard reaction Gibbs energy at temperature T and R is the ideal gas constant. Furthermore, the unimolecular reaction rate constant (k_1) employed in KiSThelP is the thermodynamic equivalent of Eq. (3):

$$k = \sigma \frac{k_b T}{h} \left(\frac{RT}{P^0} \right)^{\Delta n} e^{-\frac{\Delta G^{0,\neq}(T)}{k_b T}} \tag{3}$$

where σ is the reaction path degeneracy; k_b is Boltzmann's constant; T is the temperature; h is Planck's constant; R is the ideal gas constant and P^0 = 1 bar, with the RT/P^0 unit being the inverse of a concentration; Δn is 1 or 0 for gas-phase bimolecular or unimolecular reactions; and $\Delta G^{0,\neq}(T)$ represents the standard Gibbs free energy of activation for the reaction.

The overall rate constant can be calculated according to Eq. (4) as follows:

$$k_{overall} = K_{eq} \cdot k_1 \tag{4}$$

3 RESULTS AND DISCUSSIONS

3.1 The Formation and Decomposition of Primary Ozonides

Atomic labels are marked in the structure of citral in Fig. 1. Fig. 2 depicts the detailed reaction

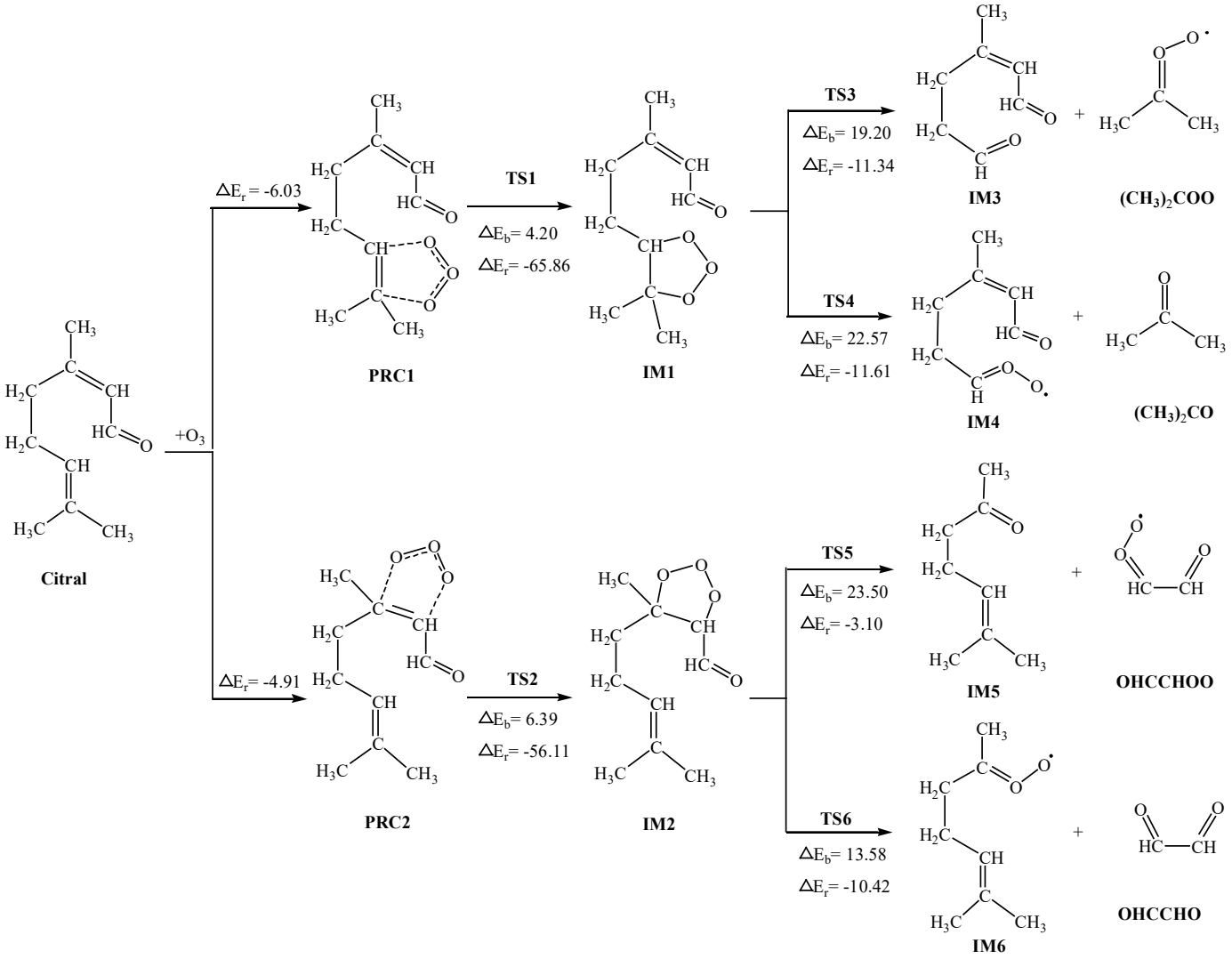

Fig. 2. The mechanisms for the formation and decomposition of primary ozonides at the M06-2X/6-311++G(3df,3pd)//M06-2X/6-31+G(d,p) level of theory (kcal mol^{-1}).

mechanism for the formation and decomposition of POZs, in which the potential barriers (ΔE_b) and reaction heats (ΔE_r) are also given. Evidently, the reaction of citral with O_3 follows the Criegee mechanism, consisting of a three-step reaction: (1) formation of PRCs, (2) electrophilic addition forming 5-member-ring primary ozonides (POZs), and (3) decomposition of POZs.

The ozonolysis of citral initiates with the addition of two terminal O atoms of O_3 to C_2=C_3 and C_7=C_8, obtaining two PRCs (PRC1 and PRC2), with the two reactions release 6.03 kcal mol^{-1} and 4.91 kcal mol^{-1} of heat, respectively. Then the POZs (IM1 and IM2) are formed through TS1 and TS2. The barrier heights of these two parallel processes are 4.20 kcal mol^{-1} and 6.39 kcal mol^{-1}, and the exothermic heat is 65.86 kcal mol^{-1} and 56.11 kcal mol^{-1}, respectively. Therefore, the reaction of O_3 with citral occurs easily under conventional atmospheric conditions.

Energized POZs have a 5-membered ring, which decomposes promptly to form carbonyl compounds [IM3, $(CH_3)_2CO$, IM5 and OHCCHO] and the corresponding CIs [IM4, $(CH_3)_2COO$·, IM6 and OHCCHOO·] through the cleavage of the C–C bond and one of the O–O bonds.

Table 1 lists the calculated rate coefficients *k* of O_3 with citral at 298 K. The predicted rate coefficient of O_3 with citral at 298 K was 6.97×10^{-17} cm^3 $molecules^{-1}$ s^{-1}, falling within the previously reported range of 10^{-19}–10^{-14} cm^3 $molecules^{-1}$ s^{-1}. Additions to C_2=C_3 bond account for more than 99% of the branching ratio and thus, further analysis focuses on the fate after addition to C_2=C_3 bond only.

Table 1. Calculated rate constants for the ozonolysis of citral and Criegee intermediate reactions.

Reactions	k_{298K} (cm^3 $molecules^{-1}$ s^{-1} or s^{-1})[a]
Citral + O_3 ⟶ PRC1 ⟶ IM1	6.92×10^{-17}
Citral + O_3 ⟶ PRC2 ⟶ IM2	4.57×10^{-20}
IM4 ⟶ DO	1.59×10^{-3}
IM4 + H_2O ⟶ HAHP	5.07×10^{-16}
IM4 + NO ⟶ IM3 + NO_2	1.58×10^{-22}
IM4 + NO ⟶ IM1-NO(2)	6.70×10^{-21}
IM4 + SO_2 ⟶ PRC-SO_2 ⟶ IM1-SO_2	3.19×10^{-10}
IM3 + O_3 ⟶ PRC3 ⟶ IM8	8.61×10^{-19}

[a] s^{-1} for unimolecular reaction, cm^3 $molecules^{-1}$ s^{-1} for bimolecular reactions.

3.2 Criegee Intermediate Reactions

The addition of O_3 to the C_2=C_3 bond will be decomposed into two CIs, $(CH_3)_2COO\cdot$ and IM4. The reactions of $(CH_3)_2COO\cdot$ have been widely investigated in recent studies (Vereecken *et al.*, 2012; Chhantyal-Pun *et al.*, 2017; Deng *et al.*, 2018). In the atmosphere, the stabilized $(CH_3)_2COO\cdot$ can undergo unimolecular isomerization reaction to form CH_2=$C(CH_3)OOH$, and can also react with SO_2, NO_2, and H_2O (Deng *et al.*, 2018). The present study focused on the fate of IM4, which may also undergo unimolecular reactions, or bimolecular reactions with water vapor and other trace gases, e.g., H_2O, SO_2 and NO_2. Fig. 3 shows the profile of the potential energy surface for the reaction of IM4. The single molecular degradation of large CIs includes the hydrogen-shift reaction, the bicyclic ring closure reactions and ring cyclization to form dioxirane (DO; Long *et al.*, 2019). Instead of intramolecular hydrogen migration and the bicyclic ring closure reactions, IM4 can undergo ring cyclization to form DO via an exothermic process and with a reaction barrier of about 22.20 kcal mol^{-1}. The rate coefficients at 298 K were estimated as 1.59×10^{-3} s^{-1}.

3.2.1 Reaction with H_2O

In atmospheric chemistry, one of the most important reactions is considered to be the reaction with H_2O because of its high abundance. Previous theoretical and experimental studies have shown that the reaction between CIs and H_2O occurs via three main reaction channels (Qi and Chao, 2007; Wang *et al.*, 2019). The pathway to produce organic peroxides is likely to be thermodynamically and kinetically advantageous compared with the other two pathways. In this channel, the H-O bond in H_2O is broken to generate OH group and H atom. The obtained OH group is attached to the C atom, while the H atom is simultaneously combined with COO· to form hydroxyalkyl hydroperoxides (HAHP). This process crosses a small potential barrier of 3.31 kcal mol^{-1} and is highly exothermic, generating 43.43 kcal mol^{-1} of energy.

For reaction with water, the rate coefficient at 298 K was estimated as 5.07×10^{-16} cm^3 $molecules^{-1}$ s^{-1} based on the TST, which is similar to the rate coefficient of 2.46×10^{-16} cm^3 $molecules^{-1}$ s^{-1} for CH_3CHOO (Wang and Wang, 2017). Theoretical studies have also shown that the reaction between $(CH_3)_2COO$ and water monomer is slow, and the rate coefficients at 298 K is 2.4×10^{-17} cm^3 $molecules^{-1}$ s^{-1} (Anglada and Sole, 2016).

When the relative humidity (RH) is 50%, the concentration of water vapor is about 3.8×10^{17} molecules cm^{-3}. Then the effective bimolecular rate is 193 s^{-1}, which is much higher than the unimolecular rate of 1.59×10^{-3} s^{-1}.

3.2.2 Reaction with NO

In the presence of NO_x, CIs can react with NO radicals, resulting in the formation of carbonyl and organic nitrate functionality. Two reaction pathways were established for the reaction between CIs and NO. The first is the formation of a 5-membered ring adduct with a nitrogen-centered radical, with a reaction barrier calculated at 9.12 kcal mol^{-1}; then step by step the C-O bond and O-O bond will break, resulting in the formation of carbonyl compounds and NO_2. The other pathway involves NO extraction of the terminal oxygen of CI, which directly generates carbonyl compounds and NO_2. The reaction barrier for this pathway is slightly higher than that of cycloaddition, at 13.58 kcal mol^{-1}.

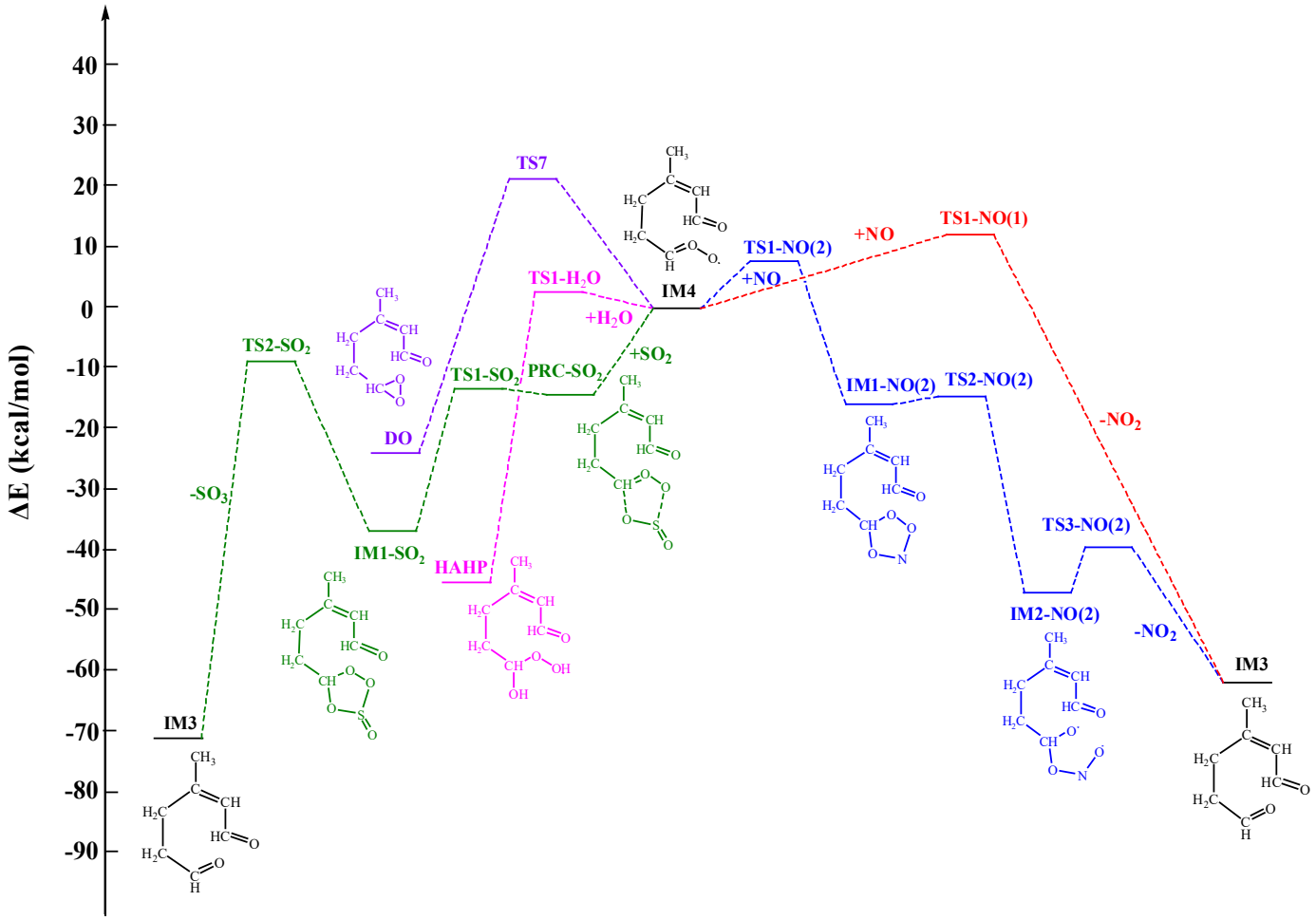

Fig. 3. The profile of the potential energy surface for the reaction of Criegee intermediates at the M06-2X/6-311++G(3df,3pd)//M06-2X/6-31+G(d,p) level of theory (kcal mol^{-1}).

Overall, it may be concluded that the reaction between CI and NO yields a carbonyl compound and NO_2, proceeding mostly through the formation of a cyclic intermediate. The NO reaction may act as a route for oxidizing NO to NO_2 in the atmosphere, affecting NO/NO_2 conversion rates. The associated NO-NO_2 cycling is particularly important for the production of tropospheric O_3 (Murray *et al.*, 2013; Newsome and Evans, 2017; Ridley *et al.*, 2017). O_3 is produced by the photolysis of NO_2 during the day, and reacts irreversibly with NO to form NO_2 at night. But the presence of CIs may compete with O_3 and reduce the reaction between NO and O_3 at night, leading to the accumulation of O_3.

The overall rate coefficient of IM4 with NO was estimated as 6.85×10^{-21} cm^3 molecules^{-1} s^{-1} at 298 K, which is 2–3 orders of magnitude lower than the estimated rate coefficient (Vereecken *et al.*, 2012). The concentrations of NO in forests, rural areas and cities are $3.3–4.8 \times 10^8$, 1.1×10^{10} and 9×10^{10} molecules cm^{-3}, respectively. Thus, the effective bimolecular rate of IM4 with NO is 2.26×10^{-12}–6.17×10^{-10} s^{-1}.

3.2.3 Reaction with SO_2

In the atmosphere, the Criegee intermediate IM4 can also undergo bimolecular reactions with SO_2, which begins with the formation of a pre-reactive complex (PRC-SO_2). This process releases 13.57 kcal mol^{-1} of energy. Then the 5-membered ring adduct IM1-SO_2 is obtained via TS1-SO_2, with this process being constrained by a reaction barrier height of 1.02 kcal mol^{-1} and being exothermic by 23.67 kcal mol^{-1}. Finally, the 5-membered ring intermediate breaks the O-O and C-O bonds to form a carbonyl compound (IM3) and SO_3. SO_3 condenses with water to form fine sulfate aerosol particles in the atmosphere, which not only affects global climate change, but also

harms human health (Sarwar *et al.*, 2013). This pathway can also account for non-OH sources in the atmosphere leading to increased sulfate aerosol production in coastal (Berresheim *et al.*, 2014) and boreal forest environments (Mauldin *et al.*, 2012).

The overall rate coefficient *k* of SO_2 with IM4 is 3.19×10^{-10} cm^3 molecules^{-1} s^{-1} at ambient temperature and 760 Torr, which is close to the previously reported experimental values of 2.4–6.7 $\times 10^{-11}$ cm^3 molecules^{-1} s^{-1} for CH_3CHOO (Taatjes *et al.*, 2013), 1.3×10^{-11} cm^3 molecules^{-1} s^{-1} for $(CH_3)_2COO$ (Huang *et al.*, 2015), and $(4.2 \pm 0.6) \times 10^{-11}$ cm^3 molecules^{-1} s^{-1} for methyl vinyl ketone oxide (Caravan *et al.*, 2020), as well as the theoretical values of $(3.68 \pm 0.02) \times 10^{-11}$ cm^3 molecules^{-1} s^{-1} for CH_2OO (Kuwata *et al.*, 2015) and 5.27–6.54 $\times 10^{-10}$ cm^3 molecules^{-1} s^{-1} for My-CIs (Deng *et al.*, 2018). The concentration ranges of SO_2 is about 1.7×10^{10} molecules cm^{-3} in the boreal forest, 9×10^{10} molecules cm^{-3} in a megacity and 6.6×10^9 molecules cm^{-3} in rural Europe (Vereecken *et al.*, 2012); thus the effective bimolecular rate of IM4 with respect to the reaction with SO_2 is about 2.11–28.71 s^{-1}. If SO_2 is present in the atmosphere at a typical level of 5×10^{11} molecules cm^{-3} (~20 ppbv) (Deng *et al.*, 2018), the effective bimolecular rate of IM4 with respect to the reaction with SO_2 is 159.5 s^{-1}.

3.3 Fate of IM3

As shown in Fig. 4, the carbonyl compound IM3 can further react with O_3, with ozone approaching the >C=C< bond forming a 5-member-ring IM8 compound via pre-reactant complexes (PRC3). This process contains a total excess energy of approximately 68.52 kcal mol^{-1}, which is sufficient to cause rapid ring breakage. The primary product channels were identified as IM9 ($CH_3COCH_2CH_2CHOO\cdot$) + *trans*-glyoxal (OHCCHO) or levulinic aldehyde ($CH_3COCH_2CH_2CHO$) + CIs ($OHCCHOO\cdot$), with potential barriers of 16.63 and 24.76 kcal mol^{-1}, respectively. The CIs $OHCCHOO\cdot$ and $CH_3COCH_2CH_2CHOO\cdot$ can further react with H_2O, SO_2 and NO to form the stabilized products glyoxal and levulinic aldehyde, respectively.

4 CONCLUSIONS

We applied quantum chemistry and kinetic calculations to identify the mechanism driving the ozonolysis of citral and gained the following insights:

1) POZs can be formed by the attachment of O_3 to C=C, after which carbonyl molecules and CIs can be formed by the simultaneous cleavage of the C-C bond of the forming 5-member-ring and one of the O-O bonds.
2) CIs can isomerize at a rate of 1.59×10^{-3} s^{-1}. Additionally, they can bimolecularly react with H_2O and SO_2 at rates of 193 s^{-1} and 159.5 s^{-1}, respectively, and, to a far lesser degree, with NO (at a rate of 2.26×10^{-12} to 6.17×10^{-10} s^{-1}). More importantly, CIs can oxidize SO_2 into SO_3, leading to the production of sulfuric acid.

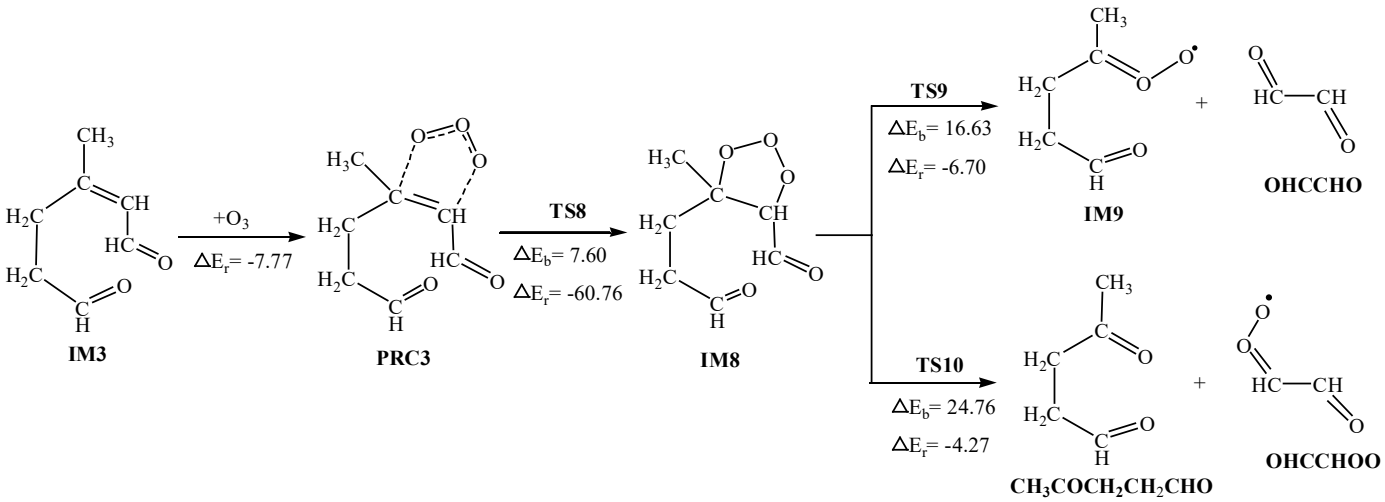

Fig. 4. The fate of IM3 with O_3 at the M06-2X/6-311++G(3df,3pd)//M06-2X/6-31+G(d,p) level of theory (kcal mol^{-1}).

The ozonolysis of citral potentially produces low-volatility species with increased water solubility, such as aldehydes [–C(=O)H], ketones [–C(=O)–], alcohols (–OH), and hydroperoxides (–OOH), which can form SOA through the nucleation, condensation, and/or partitioning of the condensed and gaseous phases.

ACKNOWLEDGEMENTS

This work is supported by National Natural Science Foundation of China (21607011, 21976109), Key Research and Development Project of Shandong Province (2019GSF109021, 2019GSF109037), and Natural Science Foundation of Shandong Province (ZR2018MB043).

SUPPLEMENTARY MATERIAL

Supplementary data associated with this article can be found in the online version at https://doi.org/10.4209/aaqr.200637

REFERENCE

Alecu, I.M., Zheng, J., Zhao, Y., Truhlar, D.G. (2010). Computational thermochemistry: Scale factor databases and scale factors for vibrational frequencies obtained from electronic model chemistries. J. Chem. Theory Comput. 6, 2872–2887. https://doi.org/10.1021/ct100326h

Almatarneh, M.H., Elayan, I.A., Altarawneh, M., Hollett J.W. (2019). A computational study of the ozonolysis of sabinene. Theor. Chem. Acc. 138, 30. https://doi.org/10.1007/s00214-019-2420-7

Anglada, J.M., Sole, A. (2016). Impact of the water dimer on the atmospheric reactivity of carbonyl oxides. Phys. Chem. Chem. Phys. 18, 17698–17712. https://doi.org/10.1039/C6CP02531E

Aplincourt, P., Ruiz-López, M.F. (2000). Theoretical investigation of reaction mechanisms for carboxylic acid formation in the atmosphere. J. Am. Chem. Soc. 122, 8990–8989. https://doi.org/10.1021/ja000731z

Atkinson, R. (1997). Gas-phase tropospheric chemistry of volatile organic compounds: 1. Alkanes and Alkenes. J. Phys. Chem. Ref. Data 26, 215–290. https://doi.org/10.1063/1.556012

Atkinson, R., Arey, J. (2003). Gas-phase tropospheric chemistry of biogenic volatile organic compounds: A review. Atmos. Environ. 37, S197–S219. https://doi.org/10.1016/S1352-2310(03)00391-1

Berresheim, H., Adam, M., Monahan, C., O'Dowd, C.D., Plane, J.M.C., Bohn, B., Rohrer, F. (2014). Missing SO_2 oxidant in the coastal atmosphere? – observations from high-resolution measurements of OH and atmospheric sulfur compounds. Atmos. Chem. Phys. 14, 12209–12223. https://doi.org/10.5194/acp-14-12209-2014

Boy, M., Mogensen, D., Smolander, S., Zhou, L., Nieminen, T., Paasonen, P., Plass-Dulmer, C., Sipila, M., Petaja, T., Mauldin, L., Berresheim, H., Kulmala, M. (2013). Oxidation of SO_2 by stabilized Criegee intermediate (sCI) radicals as a crucial source for atmospheric sulfuric acid concentrations. Atmos. Chem. Phys. 13, 3865–3879. https://doi.org/10.5194/acp-13-3865-2013

Calogirou, A., Larsen, B.R., Kotzias, D. (1999). Gas-phase terpene oxidation products: A review. Atmos. Environ. 33, 1423–1439. https://doi.org/10.1016/S1352-2310(98)00277-5

Canneaux, S., Bohr, F., Henon, E. (2014). KiSThelP: A program to predict thermodynamic properties and rate constants from quantum chemistry results. J. Comput. Chem. 35, 82–93. https://doi.org/10.1002/jcc.23470

Caravan, R.L., Vansco, M.F., Au, K., Khan, M.A.H., Li, Y.L., Winiberg, F.A.F., Zuraski, K., Lin, Y.H., Chao, W., Trongsiriwat, N., Walsh, P.J., Osborn, D.L., Percival, C.J., Lin, J.M., Shallcross, D.E., Sheps, L., Klippenstein, S.J., Taatjes, C.A., Lester, M.I. (2020). Direct kinetic measurements and theoretical predictions of an isoprene-derived Criegee intermediate. Proc. Natl. Acad. Sci. U.S.A. 117, 9733–9740. https://doi.org/10.1073/pnas.1916711117

Chhantyal-Pun, R., Welz, O., Savee, J.D., Eskola, A.J., Taatjes, C.A. (2016). Direct measurements of unimolecular and bimolecular reaction kinetics of the Criegee intermediate $(CH_3)_2COO$. J. Phys. Chem. A 121, 4–15. https://doi.org/10.1021/acs.jpca.6b07810

Deng, P., Wang, L.Y., Wang, L.M. (2018). Mechanism of gas-phase ozonolysis of β-Myrcene in the atmosphere. J. Phys. Chem. A 122, 3013–3020. https://doi.org/10.1021/acs.jpca.8b00983

Friedman, B., Farmer, D.K. (2018). SOA and gas phase organic acid yields from the sequential photooxidation of seven monoterpenes. Atmos. Environ. 187, 335–345. https://doi.org/10.1016/j.atmosenv.2018.06.003

Frisch, M.J., Trucks, G.W., Schlegel, H.B., Scuseria, G.E., Robb, M.A., Cheeseman, J.R., Scalmani, G., Barone, V., Mennucci, B., Petersson, G.A., Nakatsuji, H., Caricato, M., Li, X., Hratchian, H.P., Izmaylov, A.F., Bloino, J., Zheng, G., Sonnenberg, J.L., Hada, M., …, Fox, D.J. (2009). Gaussian 09. Revision B.01, Wallingford CT.

Gil, A., van Baren, C.M., Di Leo Lira, P., Bandoni, A.L. (2007). Identification of the genotype from contents and composition of the essential oil of lemon verbena (Aloysia citriodora Palau). J. Agric. Food Chem. 55, 8664–8669. https://doi.org/10.1021/jf0708387

Goldstein, A.H., Galbally, I.E. (2007). Known and unexplored organic constituents in the earth's atmosphere. Environ. Sci. Technol. 41, 1514–1521. https://doi.org/10.1021/es072476p

Guenther, A., Hewitt, C.N., Erickson, D., Fall, R., Geron, C., Graedel, T., Harley, P., Klinger, L., Lerdau, M., Mckay, W. A., Pierce, T., Scholes, B., Steinbrecher, R., Tallamraju, R., Taylor, J., Zimmerman, P. (1995). A global-model of natural volatile organic compound emissions. J. Geophys. Res. 100, 8873–8892. https://doi.org/10.1029/94JD02950

Hallquist, M., Wenger, J., Baltensperger, U., Rudich, Y., Simpson, D., Claeys, M., Dommen, J., Donahue, N., George, C., Goldstein, A.H., Hamilton, J.F., Herrmann, H., Hoffmann, T., Iinuma, Y., Jang, M., Jenkin, M.E., Jimenez, J.L., Kiendler-Scharr, A., Maenhaut, W., …, Wildt, J. (2009). The formation, properties and impact of secondary organic aerosol: Current and emerging issues. Atmos. Chem. Phys. 9, 5155–5236. https://doi.org/10.5194/acpd-9-3555-2009

Huang, H.L., Chao, W., Lin, J.J.M. (2015). Kinetics of a Criegee intermediate that would survive high humidity and may oxidize atmospheric SO_2. Proc. Natl. Acad. Sci. U.S.A. 112, 10857–10862. https://doi.org/10.1073/pnas.1513149112

Jackson, S.R., Ham, J.E., Harrison, J.C., Wells, J.R. (2016). Identification and quantification of carbonyl-containing α-pinene ozonolysis products using O-tert-butylhydroxylamine hydrochloride. J. Atmos. Chem. 74, 325–338. https://doi.org/10.1007/s10874-016-9344-6

Jackson, S.R., Harrison, J.C., Ham, J.E., Wells, J.R. (2017). A chamber study of alkyl nitrate production formed by terpene ozonolysis in the presence of NO and alkanes. Atmos. Environ. 171, 143–148. https://doi.org/10.1016/j.atmosenv.2017.10.002

Jaoui, M., Edney, E.O., Kleindienst, T.E., Lewandowski, M., Offenberg, J.H., Surratt, J.D., Seinfeld, J.H. (2008). Formation of secondary organic aerosol from irradiated -pinene/toluene/NO_x mixtures and the effect of isoprene and sulfur dioxide. J. Geophys. Res. 113, D09303. https://doi.org/ 10.1029/2007jd009426

Jimenez, J.L., Canagaratna, M.R., Donahue, N.M., Prevot, A.S.H., Zhang, Q., Kroll, J.H., DeCarlo, P.F., Allan, J.D., Coe, H., Ng, N.L., Aiken, A.C., Docherty, K.S., Ulbrich, I.M., Grieshop, A.P., Robinson, A.L., Duplissy, J., Smith, J.D., Wilson, K.R., Lanz, V.A., …, Worsnop, D. (2009). Evolution of organic aerosols in the atmosphere. Science 326, 1525–1529. https://doi.org/10.1126/science.1180353

Kleindienst, T.E., Edney, E.O., Lewandowski, M., Offenberg, J.H., Jaoui, M. (2006). Secondary organic carbon and aerosol yields from the irradiations of isoprene and α-pinene in the presence of NO_x and SO_2. Environ. Sci. Technol. 40, 3807–3812. https://doi.org/10.1021/es052446r

Kuwata, K.T., Guinn, E.J., Hermes, M.R., Fernandez, J.A., Mathison, J.M., Huang, K. (2015). A computational re-examination of the Criegee intermediate-sulfur dioxide reaction. J. Phys. Chem. A 119, 10316–10335. https://doi.org/10.1021/acs.jpca.5b06565

Lin, X.X., Liu, Y.R., Huang, T., Xu, K.M., Zhang, Y., Jiang, S., Gai, Y.B., Zhang, W.J., Huang, W. (2014). Theoretical studies of the hydration reactions of stabilized Criegee intermediates from the ozonolysis of β-pinene. RSC Adv. 4, 28490–28498. https://doi.org/10.1039/c4ra04172k

Long, B., Bao, J.L., Truhlar, D.G. (2019). Rapid unimolecular reaction of stabilized Criegee intermediates and implications for atmospheric chemistry. Nat. Commun. 10, 2003. https://doi.org/10.1038/s41467-019-09948-7

Martínez, E., Cabañas, B., Aranda, A. Martín, P., Salgado, S. (1999). Absolute rate coefficients for the gas-phase reactions of NO_3 radical with a series of monoterpenes at T = 298 to 433 K. J. Atmos. Chem. 33, 265–282. https://doi.org/10.1023/A:1006178530211

Mauldin, R.L., Berndt, T., Sipilä, M., Paasonen, P., Petäjä, T., Kim, S., Kurtén, T., Stratmann, F., Kerminen, V.M., Kulmala, M. (2012). A new atmospherically relevant oxidant of sulphur dioxide. Nature 488, 193–196. https://doi.org/10.1038/nature11278

Messina, P., Lathière, J., Sindelarova, K., Vuichard, N., Granier, C., Ghattas, J., Cozic, A., Hauglustaine, D.A. (2016). Global biogenic volatile organic compound emissions in the ORCHIDEE and MEGAN models and sensitivity to key parameters. Atmos. Chem. Phys. 16, 14169–14202. https://doi.org/10.5194/acp-16-14169-2016

Murray, L.T., Logan, J.A., Jacob, D.J. (2013). Interannual variability in tropical tropospheric ozone and OH: The role of lightning. J. Geophys. Res. 118, 11468–11480. https://doi.org/10.1002/jgrd.50857

Nagori, J., Janssen, R.H.H., Fry, J.L., Krol, M., Jimenez, J.L., Hu, W., Vilà-Guerau de Arellano, J. (2019). Biogenic emissions and land–atmosphere interactions as drivers of the daytime evolution of secondary organic aerosol in the southeastern US. Atmos. Chem. Phys. 19, 701–729. https://doi.org/10.5194/acp-19-701-2019

Neeb, P., Sauer, F., Horie, O., Moortgat, G.K. (1997). Formation of hydroxymethyl hydroperoxide and formic acid in alkene ozonolysis in the presence of water vapour. Atmos. Environ. 31, 1417–1423. https://doi.org/10.1016/S1352-2310(96)00322-6

Newsome, B., Evans, M. (2017). Impact of uncertainties in inorganic chemical rate constants on tropospheric composition and ozone radiative forcing. Atmos. Chem. Phys. 17, 14333–14352. https://doi.org/10.5194/acp-2017-12

Nguyen, T.B., Tyndall, G.S., Crounse, J.D., Teng, A.P., Bates, K.H., Schwantes, R.H., Coggon, M.M., Zhang, L., Feiner, P., Millller, D.O., Skog, K.M., Rivera-Rios, J.C., Dorris, M., Olson, K.F., Koss, A., Wild, R.J., Brown, S.S., Goldstein, A.H., de Gouw, J.A., …, Wennberg, P.O. (2016). Atmospheric fates of Criegee intermediates in the ozonolysis of isoprene. Phys. Chem. Chem. Phys. 18, 10241–10254. https://doi.org/10.1039/c6cp00053c

Oberdorster, G., Oberdorster, E., Oberdorster, J. (2005). Nanotoxicology: Anemerging discipline evolving from studies of ultrafine particles. Environ. Health Perspect. 113, 823–839. https://doi.org/10.1289/ehp.7339

Oliveira, R.C.D.M., Bauerfeldt, G.F. (2012). Thermochemical analysis and kinetics aspects for a chemical model for camphene ozonolysis. J. Chem. Phys. 137, 134306. https://doi.org/10.1063/1.4757150

Orlando, J.J., Barbara Nozière, Tyndall, G.S., Orzechowska, G.E., Paulson, S.E., Rudich, Y. (2000). Product studies of the OH- and ozone-initiated oxidation of some monoterpenes. J. Geophys. Res. 105, 11561–11572. https://doi.org/10.1029/2000JD900005

Pope, C.A. III, Dockery, D.W. (2006). Health effects of fine particulate air pollution: Lines that connect. J. Air Waste Manage. Assoc. 56, 709–742. https://doi.org/10.1080/10473289.2006.10464545

Presto, A.A., Huff Hartz, K. E., Donahue, N.M. (2005). Secondary organic aerosol production from terpene ozonolysis. 2. Effect of NO_x concentration. Environ. Sci. Technol. 39, 7046–7054. https://doi.org/10.1021/es050174m

Qi, B., Chao, Y.T. (2007). Theoretical study on the mechanism and kinetics of the reaction of Criegee radical CH_2O_2 with H_2O. Acta Chim. Sinica 65, 2117–2123.

Qin, M.M., Hu, Y.T., Wang, X.S., Vasilakos, P., Boyd, C.M., Xu, L., Song, Y., Ng, N.L., Nenes, A., Russell, A.G. (2018). Modeling biogenic secondary organic aerosol (BSOA) formation from monoterpene reactions with NO_3: A case study of the SOAS campaign using CMAQ. Atmos. Environ. 184, 146–155. https://doi.org/10.1016/j.atmosenv.2018.03.042

Rauber, C.S., Guterres, S.S., Schapoval, E.E.S. (2005). LC determination of citral in Cymbopogon citratus volatile oil. J. Pharm. Biomed. Anal. 37, 597–601. https://doi.org/10.1016/j.jpba.2004.10.042

Ridley, D., Cain, M., Methven, J., Arnold, S. (2017). Sensitivity of tropospheric ozone to chemical kinetic uncertainties in air masses influenced by anthropogenic and biomass burning emissions. Geophys. Res. Lett. 44, 7472–7481. https://doi.org/10.1002/2017GL073802

Saddiq, A.A., Khayyat, S.A. (2010). Chemical and antimicrobial studies of monoterpene: Citral. Pestic. Biochem. Phys. 98, 89–93. https://doi.org/10.1016/j.pestbp.2010.05.004

Sarwar, G., Fahey, K., Kwok, R., Gilliam, R.C., Roselle, S.J., Mathur, R., Xue, J., Yu, J.Z., Carter, W.P.L. (2013). Potential impacts of two SO_2 oxidation pathways on regional sulfate concentrations:

Aqueous-phase oxidation by NO_2 and gas-phase oxidation by Stabilized Criegee Intermediates. Atmos. Environ. 68, 186–197. https://doi.org/10.1016/j.atmosenv.2012.11.036

Sato, K., Jia, T., Tanabe, K., Morino, Y., Kajii, Y., Imamura, T. (2016). Terpenylic acid and nine-carbon multifunctional compounds formed during the aging of β-pinene ozonolysis secondary organic aerosol. Atmos. Environ. 130, 127–135. https://doi.org/10.1016/j.atmosenv.2015.08.047

Sauer, F., Schäfer, C., Neeb, P., Horie, O., Moortgat, G.K. (1999). Formation of hydrogen peroxide in the ozonolysis of isoprene and simple alkenes under humid conditions. Atmos. Environ. 33, 229–241. https://doi.org/10.1016/S1352-2310(98)00152-6

Scorch, C., Wissenbach, D. K., Franck, U., Wendisch, M., Schlink, U. (2017). Degradation of indoor limonene by outdoor ozone: A cascade of secondary organic aerosols. Environ. Pollut. 226, 463–472. https://doi.org/10.1016/j.envpol.2017.04.030

Shiroudi, A., Deleuze, M.S. (2014). Theoretical study of the oxidation mechanisms of naphthalene initiated by hydroxyl radicals: The H abstraction pathway. J. Phys. Chem. A 118, 4593–4610. https://doi.org/10.1021/jp500124m

Sipilä, M., Jokinen, T., Berndt, T., Richters, S., Makkonen, R., Donahue, N. M., Mauldin III, R. L, Kurten, T., Paasonen, P., Sarnela, N. (2014). Reactivity of stabilized Criegee intermediates (sCIs) from isoprene and monoterpene ozonolysis toward SO_2 and organic acids. Atmos. Chem. Phys. 14, 12143–12153. https://doi.org/10.5194/acp-14-12143-2014

Stangl, C.M., Krasnomowitz, J.M., Apsokardu, M.J., Tiszenkel, L., Ouyang, Q., Lee, S., Johnston, M.V. (2019). Sulfur dioxide modifies aerosol particle formation and growth by ozonolysis of monoterpenes and isoprene. J. Geophys. Res. 124, 4800–4811. https://doi.org/10.1029/2018JD030064

Sun, J.F., Mei, Q., Wei, B., Huan, L., Xie, J., He, M.X. (2018). Mechanisms for ozone-initiated removal of biomass burning products from the atmosphere. Environ. Chem. 15, 83–91. https://doi.org/10.1071/EN17212

Taatjes, C.A., Welz, O., Eskola, A.J., Savee, J.D., Scheer, A.M., Shallcross, D.E., Rotavera, B., Lee, E.P.F., Dyke, J.M., Mok, D.K.W., Osborn, D.L., Percival, C.J. (2013). Direct measurements of conformer-dependent reactivity of the Criegee intermediate CH_3CHOO. Science 340, 177–180. https://doi.org/10.1126/science.1234689

Truhlar, D.G., Garrett, B.C., Klippenstein, S.J. (1996). Current status of transition-state theory. J. Phys. Chem. 100, 12771–12800. https://doi.org/10.1021/jp953748q

Vereecken, L., Harder, H., Novelli, A. (2012). The reaction of Criegee intermediates with NO, RO_2, and SO_2, and their fate in the atmosphere. Phys. Chem. Chem. Phys. 14, 14682–14695. https://doi.org/10.1039/c2cp42300f

Wang, L.Y., Wang, L.M. (2017). Mechanism of gas-phase ozonolysis of sabinene in the atmosphere. Phys. Chem. Chem. Phys. 19, 24209. https://doi.org/10.1039/c7cp03216a

Wang, X., Sun, J., Bao, L., Mei, Q., Wei, B., An, Z., Xie, J., He, M.X. (2019). Mechanisms and kinetic parameters for the gas-phase reactions of 3-methyl-3-buten-2-one and 3-methyl-3-penten-2-one with ozone. J. Phys. Chem. A 123, 2745–2755. https://doi.org/10.1021/acs.jpca.8b12025

Ye, J., Abbatt, J.P.D., Chan, A.W.H. (2018). Novel Pathway of SO_2 oxidation in the atmosphere: Reactions with monoterpene ozonolysis intermediates and secondary organic aerosol. Atmos. Chem. Phys. 18, 5549–5565. https://doi.org/10.5194/acp-2017-1054

Zhang, H., Yee, L.D., Lee, B.H., Curtis, M.P., Worton, D.R., Isaacman-VanWertz, G., Offenberg, J.H., Lewandowski, M., Kleindienst, T.E., Beaver, M.R., Holder, A.L., Lonneman, W.A., Docherty, K.S., Jaoui, M., Pye, H.O.T., Hu, W., Day, D.A., Campuzano-Jost, P., Jimenez, J.L., …, Goldstein, A.H. (2018). Monoterpenes are the largest source of summertime organic aerosol in the southeastern United States. Proc. Natl. Acad. Sci. U.S.A. 115, 2038–2043. https://doi.org/10.1073/pnas.1717513115

Zheng, J.J., Zhao, Y., Truhlar, D.G. (2009). The DBH24/08 database and its use to assess electronic structure model chemistries for chemical reaction barrier heights. J. Chem. Theory Comput. 5, 808–821. https://doi.org/10.1021/ct800568m